Droplet ski-jumping on an inclined macro-textured superhydrophobic surface

Kartik Regulagadda, Shamit Bakshi, and Sarit Kumar Das

Citation: Appl. Phys. Lett. **113**, 103702 (2018); doi: 10.1063/1.5048301
View online: https://doi.org/10.1063/1.5048301
View Table of Contents: http://aip.scitation.org/toc/apl/113/10
Published by the American Institute of Physics

Droplet ski-jumping on an inclined macro-textured superhydrophobic surface

Kartik Regulagadda,[a] Shamit Bakshi, and Sarit Kumar Das[b]
Department of Mechanical Engineering, Indian Institute of Technology, Madras 600036, Tamil Nadu, India

(Received 12 July 2018; accepted 21 August 2018; published online 5 September 2018)

Rapid shedding of impinging water drops is crucial in a cold habitat for diverse reasons spanning from self-cleaning to thermal regulation in most plants, animals, and industrial applications as well. It was shown recently that deploying linear millimetric ridges on a superhydrophobic surface can reduce the contact time (for drops crashing normally) up to 50% compared to a flat surface. However, the contact time rises for drops impacting at an increasing offset to the structure. Counter-intuitively, we demonstrate a ski-jumping mechanism occurring only over a range of offsets from the macro-structure with a remarkable reduction in contact time (∼65%) during oblique impacts. Theoretically, the reduction can be as high as 80%. The flow hydrodynamics is very similar to the oblique impacts on a flat surface. However, the architecture of ridge allows the drop to rapidly fly away from the surface. This work provides new insight which can be useful for the design of surfaces with high water repellency. *Published by AIP Publishing.*
https://doi.org/10.1063/1.5048301

Reducing the droplet adhesion on a surface can be significant in multiple applications such as anti-icing,[1–5] self-cleaning,[6,7] drop-wise condensation,[8] anti-fogging,[9] and so on. Manufacturing such a surface (superhydrophobic) requires the manipulation of surface geometry at micro/nanoscale.[10,11] However, the surface wettability properties can fail under various conditions.[12–17] Conventional studies emphasize the requirement of highly dense micro/nanostructures to retain the water repellency of the surface. Richard *et al.*[18] showed that a water drop impacting a macroscopically flat superhydrophobic surface bounces off completely with a constant contact time ($\tau_s/\tau \sim 2.6$ in present experiments). Here $\tau = \sqrt{\rho R_0^3/\sigma}$ (inertio-capillary time scale), ρ is the liquid density, R_0 is the drop radius before impact, σ is the liquid-vapor interfacial tension, and τ_s represents the contact time on any particular substrate under consideration.

Recently, it has been shown that ridge-like macro-structures of similar wettability on the surface with amplitudes of the order 0.5 mm can break the hydrodynamic symmetry of impinging drops.[1,2,5] Up to 50% reduction in contact time is observed[2,5] when the impact is centered (onto the tip of the ridge) in the normal direction. However, normal impacts at increasing offset from the peak of this macro-structure will progressively produce isotropic rebound, and a rise in contact time can be observed.[1,2] In this letter, we focus on the impact of a water drop on an inclined substrate with a ridge. We show that the capability of the macro-structure to reduce the contact time degrades for oblique central impacts on the ridge. On the contrary, impacts at a particular offset from the macro-structure will produce an extremely rapid lift-off from the surface (termed as ski-jump hereafter). This mechanism exhibits up to 65% reduction in contact time for the selected experimental impact velocities. Theoretically, the reduction can be as high as 80% matching the pancake bouncing reported by Liu *et al.*[3]

The experiments in the present study are performed using high speed imaging, and the substrate used is an aluminum block ($30 \times 30 \times 10\,\text{mm}^3$) with an isosceles prism-like ridge machined using wire-cut electrical discharge machining process. It is then coated with commercially available superhydrophobic coating from Ultra ever dry. The coating renders the surface to be randomly rough as shown in the SEM image of Fig. 1. The contact angle (>160°) and roll-off angle (<5°) on the flat region (for water drops) indicate the superhydrophobic state.[11] High-performance liquid chromatography grade water drops (density $\rho = 1000\,\text{kg/m}^3$, surface tension $\sigma = 0.073\,\text{N/m}$, and radius $R_0 = 1.49 \pm 0.02\,\text{mm}$) are impacted at ten different offsets to the ridge ($0 < f < 7\,\text{mm}$). Here, f is the distance between the impact point on the surface to the ridge peak along the surface (see Fig. 1). Five

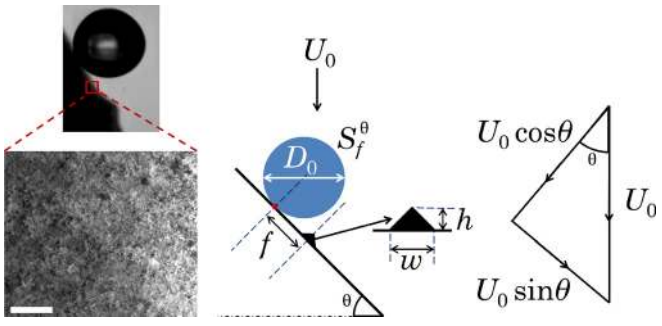

FIG. 1. The SEM image of the coated substrate and sketch of impact configuration (S_f^θ). f (in mm) indicates the distance between the impact point to the ridge tip along the surface. θ (in deg) indicates the inclination angle of the substrate with the horizontal. The cross-section of the ridge indicating its height ($h = 0.5\,\text{mm}$) and width ($w = 1\,\text{mm}$) is shown in the enlarged sketch. The normal ($U_0 \cos\theta$) and tangential components ($U_0 \sin\theta$) of the impact velocity (to the surface) are also indicated. The direction of tangential velocity is perpendicular to the axis of the ridge. The scale bar in the inset represents 1 μm.

[a]Electronic mail: kartik25192@gmail.com
[b]Current address: Department of Mechanical Engineering, Indian Institute of Technology, Ropar 140001, Punjab, India.

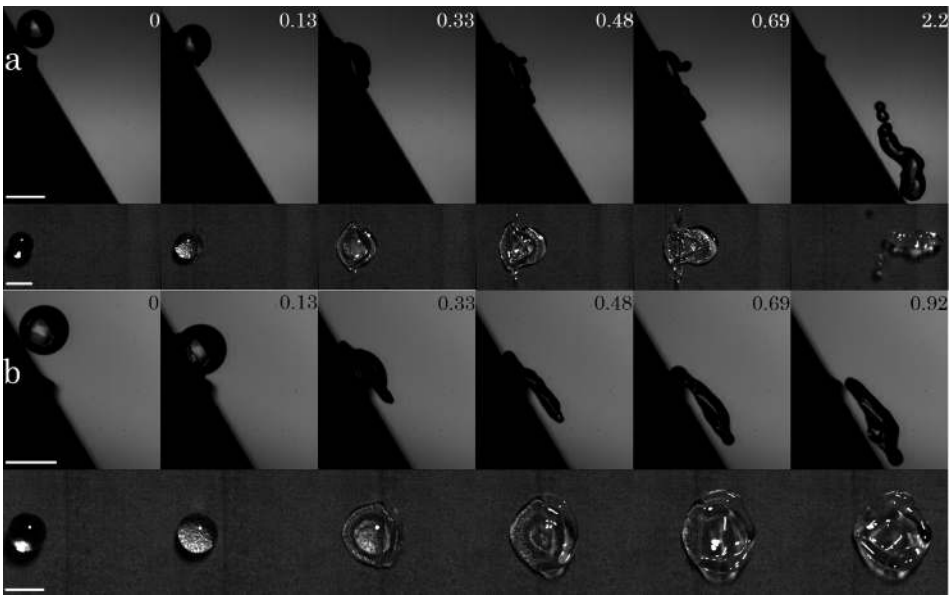

FIG. 2. Side and top views of the impact configuration (a) $S^{60^\circ}_{1.8}$, $U_0 = 1.3\,\mathrm{ms}^{-1}$, (b) $S^{60^\circ}_{3.2}$, $U_0 = 1.3\,\mathrm{ms}^{-1}$, and $R_0 = 1.49\,\mathrm{mm}$. With the only change being f in the configurations, we can observe a remarkable contact time reduction in (b) because of ski-jumping. The time indicated is non-dimensionalised with τ in each frame. The scale bars in the inset represent 3 mm. Multimedia views: https://doi.org/10.1063/1.5048301.1; https://doi.org/10.1063/1.5048301.2

different inclinations ($0^\circ \leq \theta \leq 60^\circ$) from the horizontal and four impact heights are considered for the study corresponding to Weber numbers (We) ~ 0.8, 5, 19, and 33 ($We = \rho U_0^2 R_0/\sigma$ and U_0 is the impact velocity). The side and top views are simultaneously recorded using high speed cameras at a frame rate of 8000 Hz. Hereafter, we represent any impact configuration with S_f^θ indicating the inclination angle (θ in deg) and offset from the ridge tip (f in mm) as shown in Fig. 1. It should be noted that the direction of tangential velocity is perpendicular to the direction along which the ridge is aligned. The substrates are tilted to the required angle with an accuracy of $\pm 2^\circ$ using a simple clamp mechanism.

Figure 2 shows the $S^{60^\circ}_{1.8}$ and $S^{60^\circ}_{3.2}$ configurations with $U_0 = 1.3\,\mathrm{ms}^{-1}$. In both cases, the drop slides down the surface due to the tangential momentum (M_t) and encounters the ridge during the impact. In the $S^{60^\circ}_{1.8}$ configuration [see Fig. 2(a)], the liquid continues to be in contact with the surface downhill of the ridge and the drop lifts-off from the surface at $\tau_s/\tau \sim 2.2$. However, ski-jumping takes place in the $S^{60^\circ}_{3.2}$ configuration and the liquid film detaches from the surface at the ridge tip with a strikingly reduced contact time of $\tau_s/\tau \sim 0.92$. Figure 3(a) shows the variation of non-dimensional contact time (τ_s/τ) with f for the S^{60° configuration at different We. It can be noted that there is an unanticipated fall in the contact time around $f \sim 3.2$ mm for $We \sim 19$ and 33. The pronounced reduction in contact time well below the $\tau_s/\tau \sim 1.3$ threshold of a normal impact (at ridge tip) is because of the ski-jumping phenomenon. Figure 3(b) shows the variation of τ_s/τ with f at different inclination angles (θ). One of the key features of this plot is the significant increase in contact time at smaller offsets ($f < 0.75$ mm) for $\theta \neq 0^\circ$. This means that the efficacy of the ridge pertaining to contact time reduction is downgraded during ridge-centered impact in the presence of tangential momentum (M_t). Thus, the variation in contact time with f and θ is nontrivial.

For an oblique impact, the presence of tangential momentum (M_t) significantly affects the hydrodynamics compared to the normal impacts (centered at ridge tip). For example, in the $S_0^{0^\circ}$ configuration, the hydrodynamic asymmetry redistributes the volume of the drop into multiple sub-units called lobes.[1,2,5] The morphology of the drop at the end of inertial regime takes the form of a butterfly [see the first snapshot in the inset of Fig. 3(b)]. The contact time for the $S_0^{0^\circ}$ configuration with $U_0 = 1.3\,\mathrm{ms}^{-1}$ is $\tau_s/\tau \sim 1.4$. However, during an oblique collision, the momentum distribution in different directions does not favour the formation of distinct lobes and the drop takes the shape of a pendant [see the second snapshot in the inset of Fig. 3(b)]. Thus, the contact time reduction

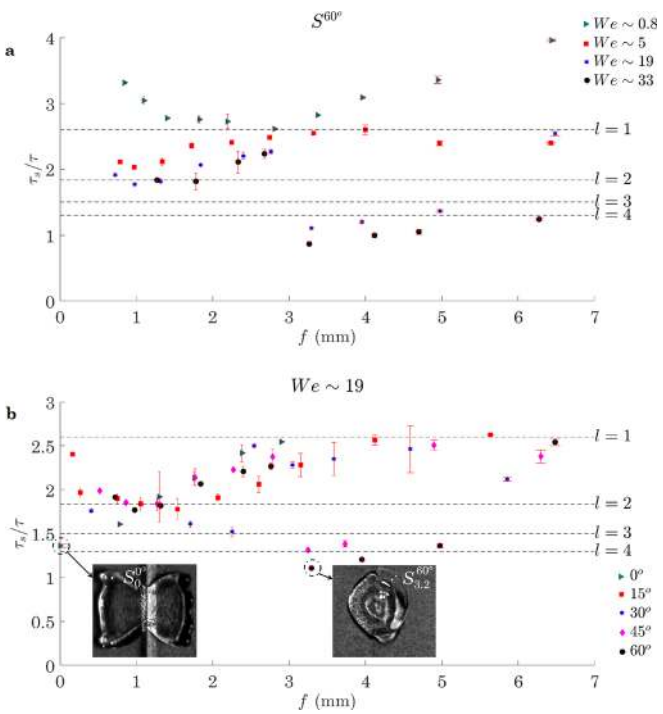

FIG. 3. (a) Plot showing the variation of non-dimensional contact time (τ_s/τ) with f at different We for the S^{60° configuration. The sharp fall in the contact time can be observed at $f \sim 3.2$ mm. (b) Plot showing the variation of τ_s/τ with f at $We \sim 19$ and different θ. The number of lobes (l) formed with $S_0^{0^\circ}$ configuration just before lift-off as mentioned by Gauthier *et al.*[2] are shown as dashed horizontal line. Snapshots in the inset show the morphology of the drop impact with $S_0^{0^\circ}$ (butterfly-like) and $S^{60^\circ}_{3.2}$ (pendant-like) at the end of inertial regime.

rather depends on the ski-jumping instead of lobe formation. The conventional idea of surface design with macro-textures hitherto dealt with maximizing the ridge-centered impacts. The results in the present work contrast this knowledge and shed new light on the impact hydrodynamics.

Two criteria are to be fulfilled for ski-jumping to occur. As explained earlier (from Fig. 2), the offset (f) plays a key role for ski-jumping for a given velocity (U_0) and substrate inclination (θ). The lamella (near the ridge) during the crash gets detached (from the surface) at the ridge tip as shown in Fig. 4(a). This ejected lamella is termed as "free" lamella hereafter. If normal momentum (M_n) on the free lamella is non-zero then, re-attachment (of liquid and solid) downhill to the ridge takes place because the normal momentum (M_n) pushes the free lamella towards the surface again as shown in Fig. 4(b). Hence, for ski-jumping, the free lamella should have zero (or negligible) normal momentum acting on it. To elucidate this, we consider the normal and tangential velocities given by $U_0 \cos\theta$ and $U_0 \sin\theta$, respectively, as shown in Fig. 1. The crash time of the drop for $We_n > 1$ scales as τ.[12,18–20] Here, We_n refers to the normal Weber number given by $We\ cos^2\theta$. The collision can be considered elastic as the restitution coefficient is close to unity.[18] Consequently, we can approximate the tangential velocity of the drop to be constant during the entire collision. Therefore, critical offset (first criterion) for ski-jumping is given by $f_{ski} \sim (U_0 \sin\theta) * C_1\tau$

$$\Rightarrow f_{ski} \sim C_1 U_0 \tau \sin\theta. \quad (1)$$

Here, the prefactor C_1 indicates the ratio of experimental crash time with the scaling time τ and is a constant whose value is close to 0.5 for $U_0 \cos\theta > 0.4\,\mathrm{ms}^{-1}$ and 0.9 otherwise. It should be noted that the minimum offset for ski-jumping is indicated by f_{ski}. An important remark here is that if $f_{ski} < R_0$, we can never have a free lamella formation because of non-zero normal momentum (M_n) of the impacting drop downhill to the ridge (see supplementary Fig. S1).

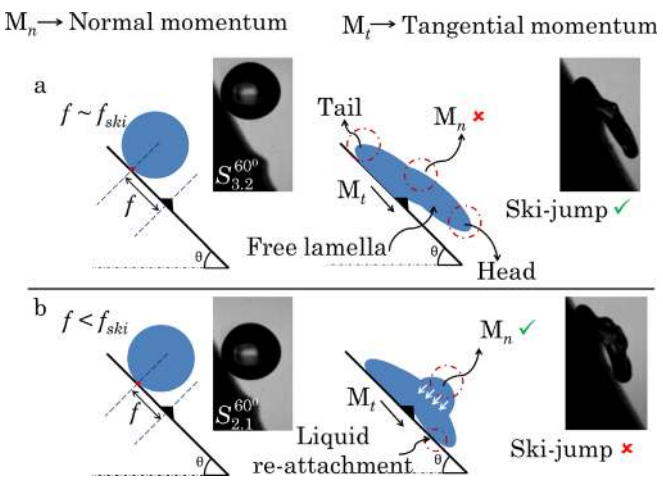

FIG. 4. Sketch to explain the first criterion for ski-jump. (a) If the offset $f \sim f_{ski}$, the normal momentum (M_n) dies out at the ridge tip making the ejected lamella "free" from the surface. Ski-jumping is possible here. The head and tail of the lamella are also indicated in the sketch. Snapshots in the inset indicate the $S^{60°}_{3.2}$ configuration at $We \sim 19$. (b) For $f < f_{ski}$, the non-zero M_n on the free lamella pushes it towards the surface (white arrows). As a result, the liquid re-attaches with the surface. Ski-jumping is not possible here. Snapshots in the inset indicate the $S^{60°}_{2.1}$ configuration at $We \sim 19$.

Thus, the first criterion can be outlined as $f \sim f_{ski} > R_0$. From now on, the usage of f_{ski} is made with an inherent assumption that $f_{ski} > R_0$. From our results, we also observe ski-jumping for a few configurations where $f > f_{ski}$. The reason for this will be clear when the second criterion is discussed. Nevertheless, it is obvious that when $f \gg f_{ski}$, the liquid may never encounter the ridge; in this case, the bouncing is similar to that on a flat surface. Hence, the scope of f is limited to a particular range for the phenomenon to take place.

From Fig. 3(a), it is clear that $f \sim f_{ski}$ is not the only criterion for ski-jumping. For $S^{60°}_{f_{ski}}$, we can observe a ski-jump at $We \sim 19$ (characterised by a sharp fall in the contact time) but not at $We \sim 5$. The second criterion of ski-jump is governed by the recoiling dynamics of the liquid film and the Worthington jet formation during the impact. For normal/oblique impacts onto macroscopically flat superhydrophobic surfaces, it is well-known that a Worthington jet emerges out from the liquid (producing a liquid column) during the recoil.[21] The time at which the jet emerges out is independent of U_0, θ, and constant for a fixed R_0 given by $t_{jet} \sim 1.3\tau$.[22,23]

The discussion hereafter assumes $f \sim f_{ski}$. From the present experiments, t_{jet} is found to be same even in the presence of a ridge. This is reasonable as the hydrodynamics with and without the ridge is approximately same apart from the formation of free lamella in the former. To elucidate the relation between ski-jumping and t_{jet}, we consider the "head" and "tail" ends of the lamella as shown in Fig. 4(a). At a time $t > t_{jet}$, the stretching of liquid column from the jet can cause a re-contact with the surface as shown in Fig. 5(a). It should be noted that the jet is bi-directional, i.e., emerges from the top and bottom of the liquid film as the lamella is

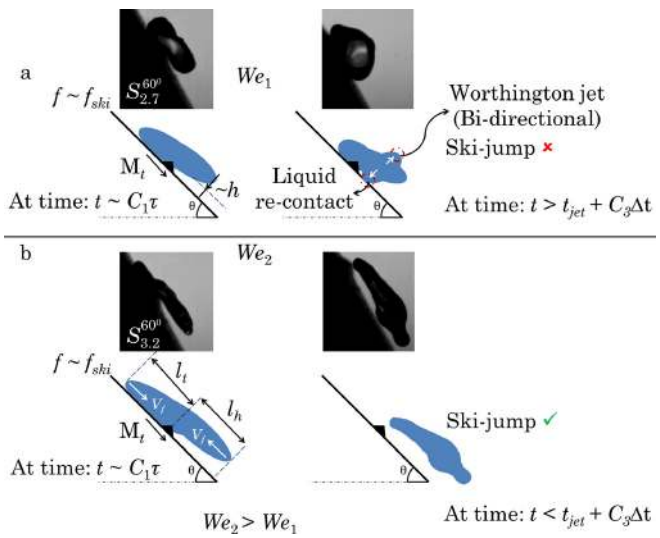

FIG. 5. Sketch to explain the second criterion for ski-jump. In both the cases, the offset $f \sim f_{ski}$. (a) Sketch showing the re-contact of the liquid emerging from the bi-directional Worthington jet at a Weber No. We_1. Here, $C_1\tau + C_2 t_{tail} > t_{jet} + C_3\Delta t$ and hence liquid re-contact takes place. The snapshots in the inset show the $S^{60°}_{2.7}$ configuration at $We \sim 5$. (b) Sketch showing the ski-jump at a Weber no. We_2 ($>We_1$). The tail detachment here is complete before the time ($t_{jet} + C_3\Delta t$), and thus we have ski-jumping. The snapshots in the inset show the $S^{60°}_{3.2}$ configuration at $We \sim 33$. l_t and l_h indicate the lamella length between the ridge to tail and head, respectively. The direction of film velocity (V_f) and tangential velocity of the drop is same at the tail and opposite at the head.

free. Thus, the detachment of the tail from the surface (at the ridge tip) should be complete before the jet re-contacts the surface to have a ski-jump; this is the second criterion. The velocity of the jet (U_{jet}) is dependent on the bubble collapse dynamics.[24] The distance between the free lamella and the surface scales as h (ridge height) as shown in Fig. 5(a). Hence, the time taken for the jet to re-contact the surface will scale as $\Delta t \sim h/U_{jet}$. The scale of U_{jet} can significantly vary with the change in $U_0 cos\theta$.[24] Hence, we can consider that U_{jet} at least scales as $U_0 cos\theta$. The tail recoiling time (t_{tail}) scales as $l_t/(V_f + U_0 \sin\theta)$, where l_t is the distance between the ridge tip and the tail at time $C_1\tau$ from the instant of impact [see Fig. 5(b)], and V_f is the film velocity. It should be noted that V_f and $U_0 sin\theta$ are in the same direction at the tail and opposite at the head. For $f \sim f_{ski}$, l_t is found to scale as R_{max} in the present experiments even though the drop shape is pendant-like. Here, $R_{max}(\sim R_0 We_n^{0.25})$ is the maximum spread radius for a normal impact on a flat surface.[20] The film velocity V_f scales as $\sqrt{2\sigma/\rho h_l}$, where h_l is the lamella thickness at maximum spread position,[25,26] and $h_l \sim 4R_0^3/3R_{max}^2$ from volume conservation. For higher tangential velocities, l_t and V_f should be calculated as explained by Almohammadi and Amirfazli.[27] From the above arguments, the second condition for ski-jumping can now be outlined as

$$(C_1\tau + C_2 t_{tail}) < (t_{jet} + C_3\Delta t). \quad (2)$$

The prefactor C_2 (~ 2) indicates the ratio of experimental tail detachment time with the scaling time t_{tail}. Likewise, C_3 (~ 0.5) indicates the ratio of experimental jet re-contact time with the scaling time Δt. Now, considering the configurations where $f > f_{ski}$, the normal momentum (M_n) will die out uphill to the ridge tip in these cases. Figure 5(b) shows l_h which is the length of the free lamella at time $C_1\tau$. Increasing f beyond f_{ski} will increase l_t and decrease l_h. The scale of l_t in these cases can be given as $R_{max} + (f - f_{ski})$. Plugging this in Eq. (2) will fetch the critical value of the offset (f_c) beyond which ski-jumping cannot take place and is given by

$$f_c = f_{ski} - R_{max} + \left[\frac{V_f + U_0 \sin\theta}{C_2}\right]\left[t_{jet} + C_3\Delta t - C_1\tau\right]. \quad (3)$$

The value of experimental critical offset ($f_{c,\exp}$) is found to be close to f_c, i.e., $f_c/f_{c,\exp} \sim 0.8$. As long as $f_{ski} < f < f_c$, we can still have a "delayed" ski-jump with an obvious rise in contact time (as l_t increases). Further increase in f ($\gg f_{ski}$) will result in no interaction of the liquid with the ridge as explained earlier. An interesting aspect of Eq. (2) is that the increase in tangential velocity ($U_0 \sin\theta$) will decrease t_{tail}. This can result in overall reduction of contact time (τ_s). To validate this argument, we performed experiments at $We \sim 73$ for a few selected configurations. We observed a contact time reduction close to 70% for the $S_{3.8}^{60^\circ}$ configuration (see supplementary Fig. S2). If $C_2 t_{tail} \ll C_1\tau$, we will have a contact time close to that of pancake bouncing reported in the literature.[3] This can happen when the tangential velocity is much greater than the normal velocity. Furthermore, the ski-jumping interval of f is dynamic and increases with higher tangential velocities (see Fig. 3).

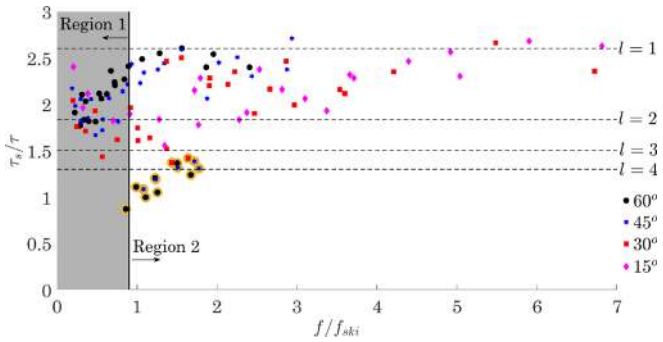

FIG. 6. Plot showing the variation of non-dimensional contact time (τ_s/τ) with offset (f/f_{ski}) for $\theta \neq 0^\circ$ at all the We. In region 1 (grey strip) we can never observe a ski-jump. The experimental transition to region 2 takes place at $f/f_{ski} \sim 0.9$ as described by the first criterion [Eq. (1)]. The data points in region 2 which are enveloped in yellow indicate the configuration where Eq. (2) is fulfilled. Thus, it is evident that when both the criteria are satisfied, we notice a ski-jump.

To summarize the key features of U_0, θ, and f, we plotted the variation of non-dimensional contact time (τ_s/τ) with f/f_{ski} in Fig. 6 for $\theta \neq 0^\circ$ at all the We. It can be noticed that the data points which fall in region 1 (grey strip) can never have a ski-jump for any U_0 and θ. Experimentally, the regional transition took place at $f/f_{ski} \sim 0.9$ as described by the first criterion [Eq. (1)]. The data points which fulfill the second criterion [Eq. (2)] are enveloped in yellow. It is clear from the plot that when both the criteria are fulfilled, ski-jumping takes place ($\tau_s < 1.3\tau$ in most cases). To further ensure the generality of the phenomenon, we have performed experiments with a drop diameter of 1.8 ± 0.01 mm. Again, we observed a similar region map as that of Fig. 6. We have also conducted experiments with substrates having multiple parallel ridges. This is important as any practical application requires multiple ridges to cater rapid shedding of all the rain drops over a large surface area. Only a particular peak-to-peak distance of the ridge allowed ski-jumping. Finally, the experiments are repeated with different cross-sectional shapes of the ridge (semi-circular and right triangle). The ski-jumping is found to be independent of the ridge shape. These results are presented in the supplementary material.

The findings in the present study can be useful in applications such as anti-icing in electrical transmission lines, air-crafts, wind turbine blades, and so on. For instance, a supercooled droplet can impact these structures in a freezing rain at any obliquity. Constructing the ridge perpendicular (rather than parallel) to the tangential velocity of the drop can significantly reduce the contact time and allows the surface to stay dry. It would be interesting to explore if similar jumping behavior is exhibited on a ridged hydrophilic surface or chemically patterned surface with a contrast of hydrophilicity and hydrophobicity on the macro-texture and background.[28,29]

See supplementary material for the details of impact movies and supplementary figures.

One of the authors, K.R., would like to thank Nikhil from IIT Tirupati for his help during the experiments.

[1]J. C. Bird, R. Dhiman, H. M. Kwon, and K. K. Varanasi, Nature **503**, 385 (2013).
[2]A. Gauthier, S. Symon, C. Clanet, and D. Quéré, Nat. Commun. **6**, 8001 (2015).
[3]Y. Liu, L. Moevius, X. Xu, T. Qian, J. M. Yeomans, and Z. Wang, Nat. Phys. **10**, 515 (2014).
[4]Y. Liu, M. Andrew, J. Li, J. M. Yeomans, and Z. Wang, Nat. Commun. **6**, 10034 (2015).
[5]K. Regulagadda, S. Bakshi, and S. K. Das, Phys. Fluids **29**, 082104 (2017).
[6]A. Marmur, Langmuir **20**, 3517 (2004).
[7]K. M. Wisdom, J. A. Watson, X. Qu, F. Liu, G. S. Watson, and C.-H. Chen, Proc. Natl. Acad. Sci. U.S.A. **110**, 7992 (2013); e-print arXiv:1406.7436.
[8]J. B. Boreyko and C.-H. Chen, Phys. Rev. Lett. **103**, 184501 (2009).
[9]T. Mouterde, G. Lehoucq, S. Xavier, A. Checco, C. T. Black, A. Rahman, T. Midavaine, C. Clanet, and D. Quéré, Nat. Mater. **16**, 658 (2017).
[10]T. Onda, S. Shibuichi, N. Satoh, and K. Tsujii, Langmuir **12**, 2125 (1996).
[11]A. Lafuma and D. Quéré, Nat. Mater. **2**, 457 (2003).
[12]D. Bartolo, F. Bouamrirene, E. Verneuil, A. Buguin, P. Silberzan, and S. Moulinet, Europhys. Lett. **74**, 299 (2006).
[13]T. Deng, K. K. Varanasi, M. Hsu, N. Bhate, C. Keimel, J. Stein, and M. Blohm, Appl. Phys. Lett. **94**(13), 133109 (2009).
[14]K. K. Varanasi, T. Deng, J. D. Smith, M. Hsu, and N. Bhate, Appl. Phys. Lett. **97**, 234102 (2010).
[15]S. Jung, M. K. Tiwari, N. V. Doan, and D. Poulikakos, Nat. Commun. **3**, 615 (2012).
[16]P. Papadopoulos, L. Mammen, X. Deng, D. Vollmer, and H.-J. Butt, Proc. Natl. Acad. Sci. U.S.A. **110**, 3254 (2013).
[17]T. Maitra, C. Antonini, M. K. Tiwari, A. Mularczyk, Z. Imeri, P. Schoch, and D. Poulikakos, Langmuir **30**, 10855 (2014).
[18]D. Richard, C. Clanet, and D. Quéré, Nature **417**, 811 (2002).
[19]K. Okumura, F. Chevy, D. Richard, D. Quéré, and C. Clanet, Europhys. Lett. **62**, 237 (2003).
[20]C. Clanet, C. Béguin, D. Richard, and D. Quéré, J. Fluid Mech. **517**, 199 (2004).
[21]A. M. Worthington, Proc. R. Soc. London **25**, 261 (1876).
[22]K. Yamamoto, H. Takezawa, and S. Ogata, Colloids Surf., A **506**, 363 (2016).
[23]K. Yamamoto, M. Motosuke, and S. Ogata, Appl. Phys. Lett. **112**, 093701 (2018).
[24]D. Bartolo, C. Josserand, and D. Bonn, Phys. Rev. Lett. **96**, 124501 (2006).
[25]G. Taylor, Proc. R. Soc. London, Ser. A **253**, 313 (1959).
[26]F. E. C. Culick, J. Appl. Phys. **31**, 1128 (1960).
[27]H. Almohammadi and A. Amirfazli, Langmuir **33**, 5957 (2017).
[28]J. A. Ritchie, J. S. Yazdi, D. Bratko, and A. Luzar, J. Phys. Chem. C **116**, 8634 (2012).
[29]U. Mock, T. Michel, C. Tropea, I. Roisman, and J. Rühe, J. Phys.: Condens. Matter **17**, S595 (2005).